Author/s:
Haghiri, A;TALEI, M;Brear, MJ;Hawkes, ER

Title:
The effect of equivalence ratio on sound generation by turbulent premixed flames

Date:
2015

Citation:
Haghiri, A., TALEI, M., Brear, M. J. & Hawkes, E. R. (2015). The effect of equivalence ratio on sound generation by turbulent premixed flames. Yang, Y (Ed.) Smith, N (Ed.) Proceedings of the Australian Combustion Symposium, pp.320-323. The Combustion Institute Australia & New Zealand Section.

Persistent Link:
https://hdl.handle.net/11343/258643

Proceedings of the Australian Combustion Symposium
December 7-9, 2015, The University of Melbourne

The effect of equivalence ratio on sound generation by turbulent premixed flames

A. Haghiri[1,*], M. Talei[1], M. J. Brear[1], E. R. Hawkes[2,3]
[1]Department of Mechanical Engineering, University of Melbourne, Parkville 3010, Australia
[2]School of Mechanical and Manufacturing Engineering, University of New South Wales, Sydney 2052, Australia
[3]School of Photovoltaic and Renewable Energy Engineering, University of New South Wales, Sydney 2052, Australia

Abstract

Direct numerical simulation (DNS) is used to study sound generation by open, turbulent premixed flames. Two cases of methane/air combustion with different equivalence ratios ($\phi = 0.7$ and 1) are considered. The computational grid is set up such that both the near and far fields are fully resolved. A simple-chemistry model is used to reduce the computational cost. The results show that flame annihilation events are significant monopolar sources of noise. Spectral analysis of the radiated sound shows a broadband spectrum where the observed frequency of the peak amplitude matches that observed experimentally. Furthermore, it is observed that the stoichiometric flame ($\phi = 1$) is a much stronger source of noise than the lean flame ($\phi = 0.7$).

Keywords: Direct numerical simulation, Combustion noise, Annihilation event, Turbulent premixed flames.

1. Introduction

In addition to being a significant form of noise pollution, combustion noise has an intimate relationship with combustion instability [1], which is a major challenge in developing low emission gas turbine combustors. Combustion instability is usually initiated by combustion-generated sound and other disturbances generated by the turbulent flame inside the combustor. The interaction of the reflected acoustic waves from the combustor's walls with the flame can introduce instability leading to failure in extreme cases. Hence, the mechanism of sound generation by turbulent flames needs to be first understood.

There are a considerable number of studies indicating that sound generation due to unsteady combustion in lean-premixed flames can lead to combustion instability, e.g. [2–8]. To develop clean and more efficient combustors, it is therefore important to address the issues associated to lean premixed flames. As a result, understanding the mechanism(s) of sound generation by premixed flames is a natural first step.

Sound generation by premixed flames has been topic of interest in the last 60 or so years. In one early study, Smith et al. [9] experimentally investigated sound generation by open turbulent premixed flames. They showed that the emitted sound originates from a distribution of monopolar sources throughout the reaction zone. This work appears to be the first to report experimentally that sound generation by a turbulent premixed flame can be essentially monopolar. They also showed that combustion noise is a broad, continuous spectrum of frequencies where its peak amplitude and associated frequency can be related to the burner diameter, the flow velocity, and the flame speed. In the same year, Bragg [10] established a simple theory to clarify the relationship between the sound production and turbulent combustion. He assumed that the generated noise is the result of changes in the flame volume or the heat release rate. It is now well established that fluctuations of the heat release rate play a significant role in generation of combustion noise, e.g. [2,3,7,8,11].

One mechanism that may result in significant fluctuations of the heat release rate is flame annihilation. Flame annihilation can occur when two flame surfaces collide with each other resulting in a rapid, unsteady consumption of the unburned gas trapped between these surfaces. There are a few experimental studies that have investigated this mechanism of combustion noise [12-14]. In a number of one- (1D) and two-dimensional (2D) numerical studies [7,8,15,16], flame annihilation has also been shown to have a significant contribution to the rate of change of heat release rate, and therefore the generated sound in laminar premixed flames. However, it is unclear whether these events are also significant sources of noise in turbulent premixed flames.

This paper therefore presents a 3D, fully-resolved DNS study of sound generation by open turbulent premixed flames. It appears that a DNS study of sound generation by an open turbulent premixed flame has not yet been reported. A simple-chemistry model is used and a comparison is made between simulations of two cases of methane-air flames with different equivalence ratios ($\phi = 0.7$ and 1), in which the premixture is preheated at T_u=800 K for both cases. The spectral content of the radiated sound is also examined with regards to experimental studies performed by others.

* Corresponding author:
Phone: (+61) 3 83446743
Email: a.haghiri@student.unimelb.edu.au

2. Computational Model

2.1 Governing Equations

Using a single-step chemistry model, the governing equations for the conservation of momentum, mass, total energy, and deficient species mass are, respectively, as follows:

$$\frac{\partial \rho u_j}{\partial t}+\frac{\partial \rho u_i u_j}{\partial x_i}=-\frac{\partial p}{\partial x_j}+\frac{\partial \tau_{ij}}{\partial x_i}, \tag{1}$$

$$\frac{\partial \rho}{\partial t}+\frac{\partial \rho u_i}{\partial x_i}=0, \tag{2}$$

$$\frac{\partial \rho E_t}{\partial t}+\frac{\partial u_j(\rho E_t+p)}{\partial x_j}=\frac{\partial u_i \tau_{ij}}{\partial x_j}-\frac{\partial q_j}{\partial x_j}, \tag{3}$$

and

$$\frac{\partial \rho Y_F}{\partial t}+\frac{\partial \rho u_j Y_F}{\partial x_j}=\frac{\partial}{\partial x_j}\left(\rho D\frac{\partial Y_F}{\partial x_j}\right)-\dot{\omega}_F, \tag{4}$$

where x and t are the spatial coordinate and time, respectively. In addition, ρ is the density, u_j is the j-component of flow velocity, Y_F is the fuel mass fraction, p is the pressure, E_t is the total energy per unit mass (internal energy plus kinetic energy), q_j is the heat flux vector considering constant heat capacity, and τ_{ij} is the ij-component of the viscous stress tensor. The quantities E_t , q_j and τ_{ij} are given by,

$$E_t=\frac{p}{\rho(\gamma-1)}+Y_F Q+\frac{1}{2}u_i u_i, \tag{5}$$

$$q_j=-\lambda\frac{\partial T}{\partial x_j}-\sum_{k=1}^{N_s=2}\left(\Delta h_k^0\rho D\frac{\partial Y_k}{\partial x_j}\right), \tag{6}$$

$$\tau_{ij}=\mu\left[\frac{\partial u_i}{\partial x_j}+\frac{\partial u_j}{\partial x_i}-\frac{2}{3}\frac{\partial u_k}{\partial x_k}\delta_{ij}\right], \tag{7}$$

where γ is the heat capacity ratio, Q is the heat of reaction per unit mass of reactant, Δh_k^0 is the chemical enthalpy of formation evaluated at reference temperature T_0, μ is the dynamic viscosity, D is the binary mass diffusion coefficient, λ is the mixture thermal conductivity, and δ_{ij} is the Kronecker delta. The fuel reaction rate $\dot{\omega}_F$ may be obtained using the Arrhenius law as follows:

$$\dot{\omega}_F=\Lambda\rho Y_F\exp\left[-\frac{\beta(1-\theta)}{1-\alpha(1-\theta)}\right], \tag{8}$$

where

$$\Lambda=B\exp(-\beta/\alpha),\ \theta=\frac{T-T_0}{T_f-T_0}, \tag{9}$$

$$\alpha=\frac{T_f-T_0}{T_f},\ and\ \beta=\frac{E_a(T_f-T_0)}{RT_f^2}. \tag{10}$$

Note that B is the pre-exponential factor, β is the Zel'dovich number, T_f is the adiabatic flame temperature, T_0 is the fresh mixture temperature at jet inlet, E_a is the activation energy, R is the universal gas constant, and α is the heat release parameter.

2.2 Numerical Method

Direct numerical simulation (DNS) of the governing equations (1-4) was carried out using a modified version of the code S3D [17] (referred to as S3D-SC [18]) which features an 8th order central differencing scheme for spatial derivatives, combined with a 4th order explicit Runge–Kutta time integrator. S3D is an MPI-compatible solver and can be run on parallel processors with a high performance.

Figure 1 shows a schematic of the computational domain. The computational domain was resolved using a 3D structured Cartesian mesh. The boundary conditions were based on 3D Navier-Stokes Characteristic Boundary Condition (3DNSCBC) [19]. All boundaries were carefully treated to avoid spurious noise reflections.

A subsonic round jet of unburned premixed mixture (reactant) is injected into an open environment of adiabatic combustion products. The environment's temperature is equal to the product temperature. Two cases of methane/air combustion were considered with different equivalence ratios (ϕ = 0.7 and 1), in which the reactants are preheated at T_u=800 K in both cases. A coflow with a low velocity magnitude (1% of the jet mean velocity) surrounds the jet flame at the product temperature to mimic natural convection around jet flames in real conditions. The simulation parameters for both cases are presented in Table 1.

The mean inlet streamwise velocity was adapted from the DNS study of Wu and Moin [20] where a fully developed turbulent pipe flow at the Reynolds number Re_D=5300 was simulated. To impose the velocity fluctuations at the inlet boundary, homogeneous isotropic turbulence, obtained based on the Passot-Pouquet energy spectrum [21] with a centreline turbulence intensity of 3.7 %, was first generated. The velocity fluctuations at the inlet were then obtained by rescaling the streamwise velocities of the turbulence field with the turbulence intensity profile of the pipe flow simulation in the streamwise direction [20]. The resulting frozen velocity field was then added to the mean inlet velocity using the Taylor hypothesis.

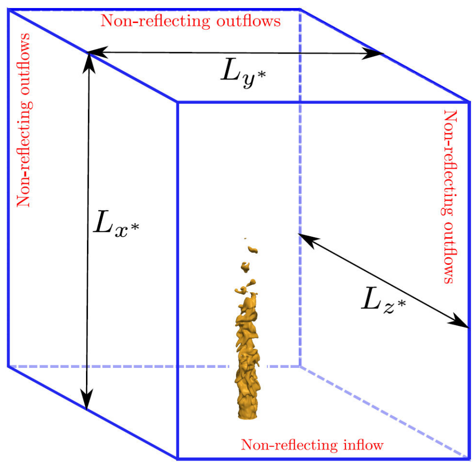

Figure 1: The computational domain (not to scale).

Table 1: The simulation parameters used in the present study.

	$\phi = 1$	$\phi = 0.7$
Jet diameter	D	
Domain size	20D × 16D × 16D	
Grid resolution	2412 × 1040 × 1040	
Mean inlet jet Mach number	0.35	0.26
co-flow Mach number	0.0035	0.0026
Heat release parameter (α)	0.675	0.637
Jet Reynolds number (Re)	5300	5300
δ_{th} / D	0.07	0.07
S_L / a_{ref}	0.00422	0.00325
β	7.9	5.5
Pr	0.72	0.72
Le	1.0	1.0

The simulations for both cases were performed using a constant time step for six complete jet flow-through times to achieve a statistically stationary solution. The data of the last four flow-through times were used for post-processing.

3. Results and Discussion

3.1 Flame-Generated Sound and Related Acoustic Field

Instantaneous snapshots of the temperature and dilation fields ($(D/a_{ref})\nabla.\vec{u}$) extracted at the central X-Y plane through the jet are shown in Fig. 2 for each case. (It can be readily shown that the dilatation and the pressure are related in the far field [22]). Flame annihilation evidently occurs, in particular near the flame tip. Looking at the dilatation fields, it can be seen that the acoustic fields for both the stoichiometric and lean flames feature discrete monopolar sound sources. The sound produced from these sources, originating some distance downstream of the nozzle, clearly dominate the incoming noise at the inflow.

It should be also noted that weaker monopolar sources of sound appear in the lean flame. Since both simulated cases have the same Reynolds numbers and turbulence intensities, this observation is most likely related to a difference in chemical parameters, such as flame speeds, between two cases. However, a more detailed analysis is required to quantify the contribution of annihilation events and the role of the flame key parameters to the overall radiated sound.

3.2 Spectral Analysis

The spectrum of the produced sound is calculated on a plane perpendicular to the jet axis at x/D=10. Eight uniformly-distributed virtual microphones at r/D=6 are placed on the plane to measure the sound intensity. The mean frequency spectrum is then obtained by averaging the spectrum of all individual microphones. To reduce the so-called 'spectral leakage' and to obtain the smallest spectral variance per data point, a modified Hanning window [23] with 50% overlap [24] was used to perform the fast Fourier transform (FFT) at each probe.

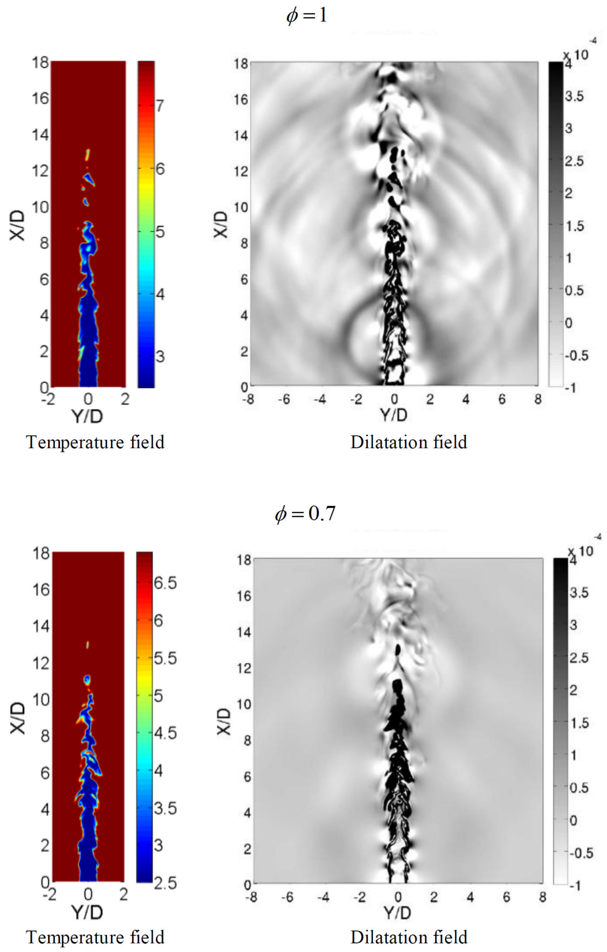

Figure 2: The instantaneous dimensionless temperature and dilatation fields for each case.

The averaged calculated spectrum for each case is shown in Fig. 4. Similar to earlier experimental studies (e.g [25]), the produced sound is broadband in nature in our study. Furthermore, the magnitude of the noise radiated by the stoichiometric flame is significantly greater than that of the lean flame.

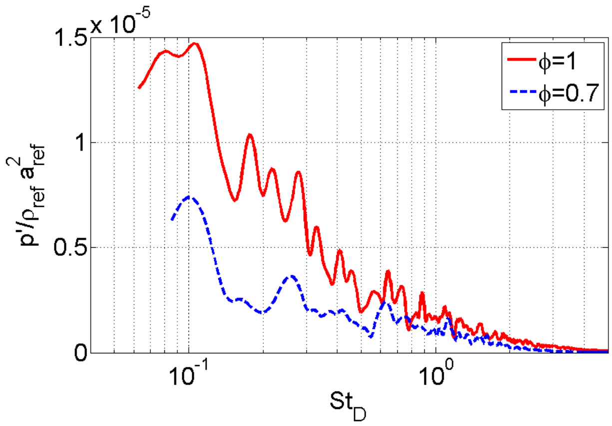

Figure 3: The calculated noise spectrum for each case at x/D=10, r/D=6. The horizontal axis shows Strouhal number (St_D=fD/U_{av}) and the vertical axis shows the non-dimensional acoustic pressure.

Rajaram and Lieuwen [25] investigated noise generation by a number of turbulent premixed flames and found that the frequency of peak emissions f_{peak} across all burners, flow velocities, fuel/air ratios, and fuel types, is mainly a function of the flame length and the mean inlet velocity. They calculated the flame length based on the variance of every pixel in the intensity of chemiluminescence emitted by the flame. This intensity was regarded as a measure of the heat release at that location. The flame length L_{flame} was then defined as the distance between the heights where the horizontally integrated intensity of the variance image crosses a quarter of the maximum value. They showed that the peak Strouhal number ($St_{peak} = f_{peak} L_{flame} / U_{av}$) is close to unity for the experimental conditions that they tested.

In the present study the flame length was calculated using the variance of the reaction rate field by following the method proposed by Rajaram and Lieuwen [25]. The flame lengths were approximately equal to 12.8D and 11.8D for the stoichiometric and lean cases, respectively. Using these values for the flame lengths, the peak Strouhal numbers for the stoichiometric and lean flames are equal to 1.3 and 1.2, respectively. These values therefore agree well with the peak Strouhal numbers found experimentally [25].

4. Conclusion

This paper presented a direct numerical simulation (DNS) study of sound generation by turbulent premixed flames. Two cases of methane/air flames with different equivalence ratios ($\phi = 0.7$ and 1) were considered. A single-step chemistry model was used to reduce the computational cost. Care was taken to fully resolve both the near and far fields and avoid spurious reflections at the outflow boundaries using the three dimensional Navier-Stokes Characteristic Boundary Condition (3D-NSCBC).

It was observed that the interaction of flame surfaces led to flame annihilation events, specifically in the downstream region near the flame tip. The acoustic fields for both the stoichiometric and lean flames also featured discrete monopolar sound sources originating from these annihilation events, with the strength of these sources clearly dependent on equivalence ratio. The spectra of the radiated noise were then examined. These were found to be broadband in nature, with a frequency of the peak amplitude that follows the scaling proposed by Rajaram and Lieuwen [25].

A more detailed analysis is required to quantify the contribution of annihilation events and the flame key parameters to the overall radiated sound. This is a topic of our future research.

5. Acknowledgments

This study was supported by the Advanced Centre for Automotive Research and Testing (ACART, www.acart.com.au), the Australian Research Council (ARC) and the National Computational Merit Allocation Scheme, supported by the Australian Government. The computational facilities supporting this project included the Australian National Facility (NCI), the partner share of the NCI facility provided by Intersect Australia Pty Ltd., the Peak Computing Facility of the Victorian Life Sciences Computation Initiative (VLSCI) and iVEC (Western Australia).

6. References

[1] N. Swaminathan, K. N. C. Bray, (Eds.) Turbulent premixed flames. Cambridge University Press, 2011.

[2] I.R. Hurle, R.B. Price, T.M. Sugden, A. Thomas, Proc. R. Soc. Lond. A **303** (1968), pp. 409–427.

[3] W.C. Strahle, Prog. Energy Combust. Sci. **4** (1978), pp. 157–176.

[4] D.G. Crighton, A.P. Dowling, J.E. Ffowcs Williams, M. Heckl, F.G. Leppington, Modern Methods in Analytical Acoustics: Lecture Notes, Springer-Verlag, London, 1992.

[5] N. Swaminathan, R. Balachandran, G. Xu, A.P. Dowling, Proc. Combust. Inst. **33** (2011), pp. 1533–1541.

[6] N. Swaminathan, G. Xu, A.P. Dowling, R. Balachandran, J. Fluid Mech. **681** (2011), pp. 80–115.

[7] M. Talei, M.J. Brear, E.R. Hawkes, J. Fluid Mech. **679** (2011), pp. 194–218.

[8] M. Talei, M.J. Brear, E.R. Hawkes, Combust. Flame **159** (2) (2012), pp 757–769.

[9] T.J.B Smith, T. J. B., J.K Kilham, J. Acoust. Soc. Am. **35** (1963), pp. 715-724.

[10] S.L Bragg, J. Inst. Fuel **36** (1) (1963), pp. 12-16.

[11] C.K. Tam, Int. J. Aeroacoust., **14**(3-4) (2015), pp. 431-456.

[12] N. Kidin, V. Librovicht, J. Roberts, M. Vuillermoz, Dyn. Flames React. Syst. (1984), pp. 343–355.

[13] T. Schuller, D. Durox, S. Candel, Combust. Flame **135** (2003), pp. 525–537.

[14] S. Candel, D. Durox, T. Schuller, in: 10th AIAA/ CEAS Aeroacoustics Conference, Paper No. 2004- 2928, pp. 1444–1454.

[15] M. Talei, M.J. Brear, E.R. Hawkes, Proc. Combust. Inst. **34** (1) (2012), pp. 1093–1100.

[16] C. Jiménez, A. Haghiri, M.J. Brear, M. Talei, E.R. Hawkes, Proc. Combust. Inst. **35**(3) (2015), pp. 3317-3325.

[17] J.H. Chen, A. Choudhary, B. De Supinski, M. Devries, E.R. Hawkes, S. Klasky, W.K. Liao, K.L. Ma, J. Mellor-Crummey, N. Podhorszki, R. Sankaran, S. Shende, C.S. Yoo, Comput. Sci. Discovery **2** (2009), 015001.

[18] S. Karami, E.R. Hawkes, M. Talei, J.H. Chen, J. Fluid Mech. **777** (2015), pp. 633- 689.

[19] C.S. Yoo, H.G. Im, Combust. Theor. Model., **11**(2) (2007), pp. 259-286.

[20] X. Wu, P. Moin, J. Fluid Mech. **608** (2008), pp. 81-112.

[21] T. Passot, and A. Pouquet, J. Fluid Mech., **181** (1987), pp. 441–466.

[22] T. Colonius, S.K. Lele, P. Moin, J. Fluid Mech., **330** (1997), pp. 375–409.

[23] D.P. Lockard, J. Sound Vib. **229**(4) (2000), pp. 897–911.

[24] T.P. Bui, W. Schröder, M Meinke,. Comput. Fluids **37**(9) (2008), pp. 1157-1169.

[25] R. Rajaram, T. Lieuwen, J. Fluid Mech. **637** (2009), pp. 357–385.